FATIGUE DAMAGE AND ITS NONDESTRUCTIVE EVALUATION: AN OVERVIEW

Otto Buck

Ames Laboratory and Materials Science and Engineering Department
Iowa State University
Ames, IA 50011

INTRODUCTION

This paper deals with the basic mechanisms of fatigue damage in materials exposed to service and a series of nondestructive techniques for the early detection of this damage. For all materials with reasonably high fracture toughness it is the organized motion of dislocations that either forms extrusions/intrusions (surface roughness) or the piling up of dislocations at grain boundaries or interface boundaries whose unzipping forms small cracks. Some of these small cracks grow, coalesce with other small cracks and eventually form the large crack which will terminate the life of the structure, if it grows to a size that is large enough (at a given stress level) to reach the fracture toughness of the material. The time scale of these events is roughly: First small cracks ($a \approx 0.1\mu m$) initiate at $\approx 10\%$ of the total life; large cracks appear ($a \approx 0.5mm$) at $\approx 90\%$ of the total life. Details depend on the microstructure of the material, the applied stress and other environmental factors. Over the past thirty years, researchers have tried to follow this sequence of events with a variety of experimental techniques that are adjusted to the specific defect type to be detected (dislocations, small cracks, and large cracks). Some of these techniques are briefly reviewed.

FATIGUE DAMAGE

Constant Amplitude Cycling

The most simplistic definition of fatigue damage is given by the number of fatigue cycles applied (N) to a given material divided by the number of cycles to failure (N_f) where N_f is that point in the strain-life (S-N) curve where 50% of the specimens have failed. S is either the stress or the strain amplitude applied, as indicated in Fig. 1. Starting with a smooth bar specimen without any stress concentrations, one may define [1] N_f as the sum of the number of cycles to fatigue crack initiation (N_i) plus the number of cycles (N_{sc}) the small crack needs to grow into a large crack plus the number of cycles (N_{lc}) the large crack needs to grow to the catastrophic crack size (or K_{Ic} or J_{Ic}),

$$N_f = N_i + N_{sc} + N_{lc}. \quad (1)$$

N_f for metals follows basically a log normal distribution, whereas in ceramics a Weibull distribution is more appropriate. Note that the log normal distribution is basically just a special case of the Weibull distribution.

The definition of N_i is complex and depends to a large degree on the question: "When is a crack a crack?" The NDE community believes that a small crack has been developed as soon as it is detectable by ultrasonics or eddy current or any other NDE technique. Thus, at the present time a small crack would be a few tenths of a mm in depth (a) and width (2c) in Fig. 2. A scanning electron microscope (SEM), on the other hand, will detect cracks with dimensions on the order of a few micrometers [2]. Thus, the SEM detects cracks at about 10% of

Review of Progress in Quantitative Nondestructive Evaluation, Vol 17
Edited by D.O. Thompson and D.E. Chimenti, Plenum Press, New York, 1998

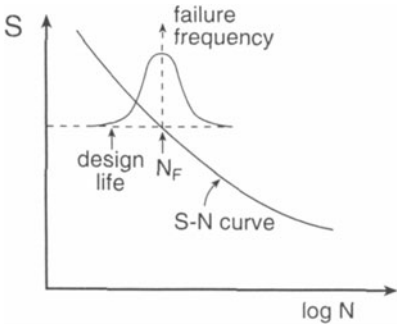

Figure 1. Probability of failure in relation to the S-N curve. S could be either the stress or the strain amplitude.

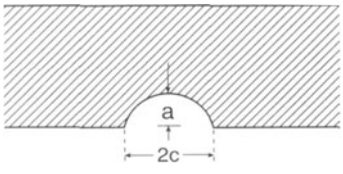

Figure 2. Definition of crack dimensions.

N_f, and typical NDE techniques at about 50% of N_f. These values for N_i depend strongly on the stress or strain amplitude applied, on the microstructure as well as environmental influences (stress corrosion cracking). The application of the atomic force microscope (AFM) to these problems may be of particular interest.

As soon as a small crack has been observed the question arises: "How fast is it growing?" Usually one expresses the fatigue crack growth in terms of da/dN, which is the change in crack length per fatigue cycle, versus the stress intensity range, ΔK, given by the "driving force"

$$\Delta K = K_{max} - K_{min} \tag{2}$$

where $K_{max} = g\sigma_{max}\sqrt{\pi a}$ and $K_{min} = g\sigma_{min}\sqrt{\pi a}$ with σ_{max} being the maximum cyclic stress applied and $K_{min} = 0$ during the compression part of the cycle ($\sigma_{min} < 0$) (see Figure 3), and g a geometry factor. Similar arguments have been advanced if the material shows some ductility. One such example is crack initiation at a notch where a plastic zone is created. The driving force is then best described by J which is roughly $J \approx K^2/E$. However, for cracks initiated at some microstructural feature on a smooth surface, Equation (2) is applied [3].

The density of small cracks at initiation depends strongly on the stress or strain amplitude. As Kitagawa et al. [4] observed, at high stress amplitudes (the low cycle fatigue regime) there are about 6 cracks/mm^2 initiated; at low stress amplitudes (the high cycle fatigue regime), about 1 crack/mm^2 is initiated. For a definition of low and high cycle fatigue regimes, see Fig. 4. If the fatigue is conducted under strain amplitude ($\Delta\varepsilon/2$) control, the strain-life relationship (S-N) is mathematically formulated as

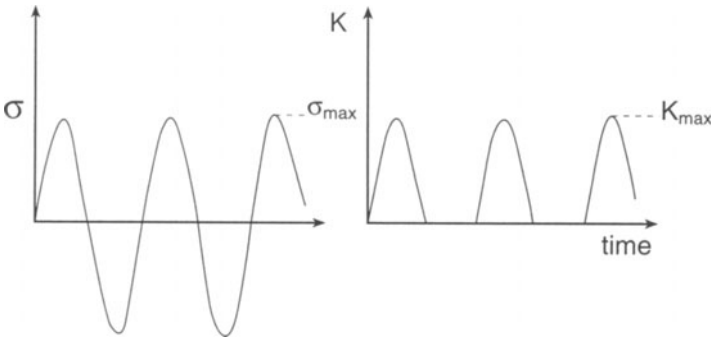

Figure 3. The stress applied to the specimen as a function of time.

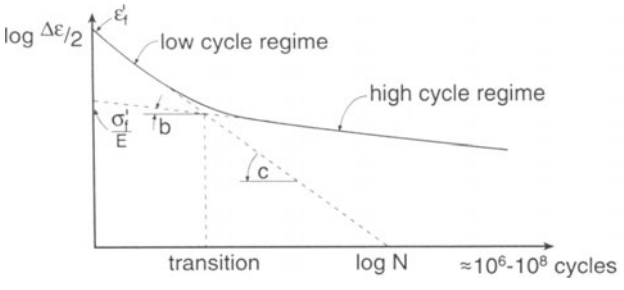

Figure 4. Definition of low and high cycle fatigue.

$$\frac{\Delta\varepsilon}{2} = \frac{\sigma_f'}{E}(N)^b + \varepsilon_f'(N)^c \tag{3}$$

with $\frac{\sigma_f'}{E}(N)^b$ describing the high cycle and $\varepsilon_f'(N)^c$ describing the low cycle behavior [5].

After initiation, which will be discussed in more detail in the next chapter, the small cracks propagate relatively fast for some period of time and then get either arrested or retarded at grain boundaries or other obstacles. The retarded ones will resume their accelerated growth and eventually join the crack growth rate for large cracks (Paris regime) at about 90% of N_f expressed as

$$\frac{da}{dN} = A(\Delta K)^m \tag{4}$$

where A and m are materials parameters and ΔK is given by Equation (2). Final failure is achieved when $\Delta K \approx K_{Ic}$ where K_{Ic} is the fracture toughness. At that point damage is defined to be equal to one.

MICROMECHANISMS OF SMALL CRACK INITIATION

If we want to monitor the fatigue damage done to the specimen we have to know what the defects are that are indicative of the particular state of the damage. These are either point defects, dislocations, small cracks or large cracks. In the following we will briefly discuss these defects and their role in fatigue.

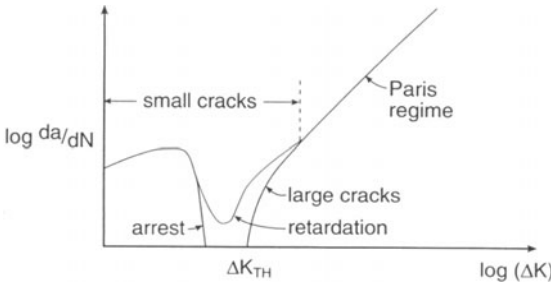

Figure 5. Crack growth rate for small cracks and its convergence into the Paris regime for large cracks (after Ref. 3).

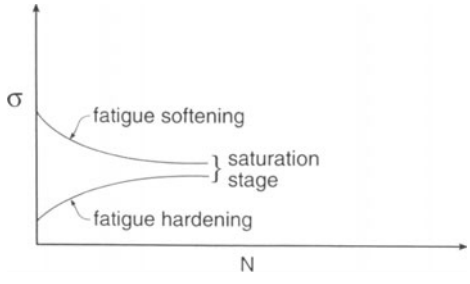

Figure 6. Flow stress as a function of fatigue cycles. a) Hardening. b) Softening.

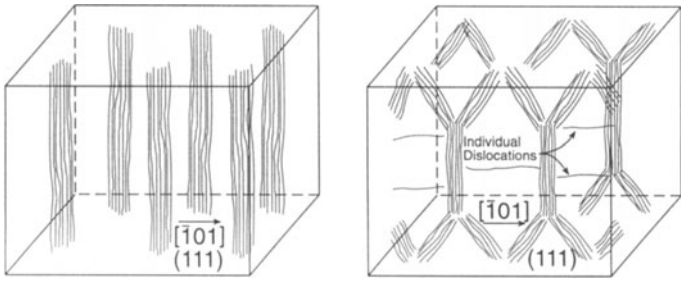

Figure 7. Dislocation configurations developed during fatigue. a) Sketch of dislocation bundles. b) Cell structure with individual dislocations.

Dislocation Effects

Dislocations are certainly the major active players before fatigue crack initiation occurs [6,7]. In fcc single crystals, during the so-called fatigue hardening stage which is the early stage of fatigue (Fig. 6), bundles of dislocations are formed which are separated by regions which are relatively free of dislocations [6]. The bundles tend to be oriented perpendicular tothe primary Burgers vector, as sketched in Fig. 7a. As hardening continues, the average spacing between bundles decreases. In other words, the average dislocation density in-

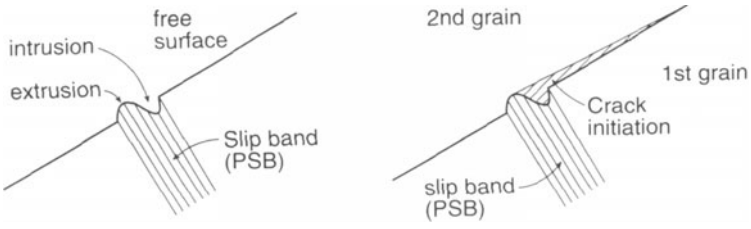

Figure 8. Roughness formed by persistent slip bands. a) At a free surface. b) At a grain boundary.

creases. At the same time, the electrical resistivity increases which is a consequence of both, the dislocation density as well as the point defect (vacancy) concentration increase.

At the beginning of the so-called saturation stage, the well defined bundles break up to form a "cell structure", sketched in Fig. 7b. Again the interior of the cells is almost dislocation-free. However, slip bands form at the surface, as shown in Fig. 8a, which spread inward. The slip bands (often referred to as persistent slip bands) form a roughness on the surface (Fig. 8a) that develops into extrusions and intrusions, with the intrusions forming thesite of small crack initiation. Responsible for the slip band formation is the shuttling forth and back of the individual dislocations in Fig. 7b.

Note that the discussion so far centered around single crystals. Research on single crystals is important to commercial alloys in that initiation usually occurs in a single grain and is often confined to the primary glide plane (just as in single crystals), under an angle of closeto 45° to the stress direction, as required by the Schmid factor. In terms of crack initiation, this type of initiation is called "Stage I" initiation.

In polycrystalline alloys, similar dislocation mechanisms appear to be effective concerning small crack initiation. For instance in high strength aluminum alloys, slip bands within a grain are piling up dislocations against intermetallic particles and fracture the particles [8] or the phase boundary between the matrix and the particle [9]. Similar observations are made on Inconel 718 [10] and many other industrial alloys (see Reference 2, e.g.). Another possibility is that the slip bands pile up against grain boundaries. If the grain boundaries are embrittled by certain impurities, the grain boundaries open up, forming a small crack [11] as sketched in Fig. 8b.

Cycling About a Bias Stress and with Changing Amplitude

In the real world, fatigue cycling hardly ever looks like given in Fig. 3. Usually a bias stress is superimposed or rapid changes from low to high cycle fatigue are present, such as indicated in Fig. 9. Bias stresses mainly shift the high cycle fatigue curve, affecting the life of

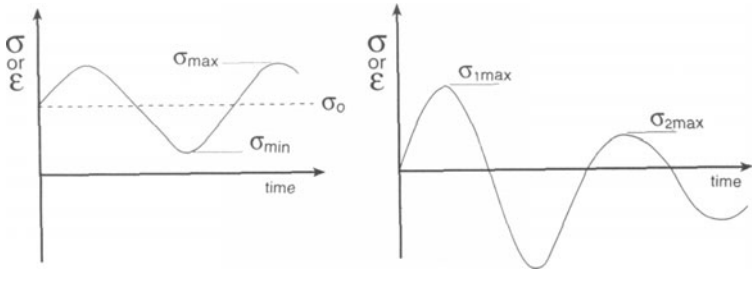

Figure 9. Examples of complex fatigue spectra. a) Bias stress or strain. b) Transition of low to high cycle fatigue.

the specimen in a positive or negative way (a compressive stress extends the life, e.g.). Transitions from low to high cycle fatigue (and vice versa) are accounted for by the well-known "rain flow method" which provides rules on which of the fatigue cycles contribute to the damage, done in a particular cycle. As far as this author knows, detailed studies on crack initiation under such complex spectra have not been performed as yet.

CRACK SIZE DISTRIBUTIONS AND PROPAGATING SMALL CRACKS

In single crystals, cracks are initiated at intrusions of a depth of about 0.1μm or less along the favored slip plane [2]. In polycrystalline materials, one observes crack coalescence (one small crack combining with another one) which leads to bimodal crack size distributions [9]. The reason is that small cracks grow very fast until they are stopped by grain boundaries that have a different grain orientation than the original grain. If the grain size is reasonably homogeneous it is then not surprising to find crack lengths of multiples of the grain size. An interesting study of the crack size distribution in stage I as a function of fatigue cycles applied has been performed by Ma and Laird [12] who made their observations on a large number of cracks. The number of cracks per unit area becomes larger with fatigue cycling. The distributions are heavily skewed to the smaller crack sizes and are close to log normal. The larger cracks become even larger with increasing fatigue cycle numbers.

As Lankford and Davidson [3] noted, small cracks grow at unexpectedly fast rates (da/dN), particularly if their plastic zone sizes are small with respect to the grain size. Small cracks can be either arrested at grain boundaries (or other obstacles) or retarded for a number of fatigue cycles before reinitiation in the next grain occurs (see Fig. 5). Eventually they join the Paris regime of long cracks and then propagate according to Equation 4. Note that according to Ref. 1 both small and long crack growth is, to some degree, dominated by "crack closure"[13]. However, crack closure alone is not sufficient to produce one single growth law, such as given by Equation 4. Obviously, the crystallographic orientation of the grain into which the small crack grows is also responsible for the crack growth rate (a change of the Schmid factor). For more details on crack closure and how to measure it acoustically, see Ref. 14. A Monte Carlo simulation of small crack initiation and growth was performed by Morris et al. [15] describing the initiation and growth as well as the median life (Fig. 1) reasonably well.

MATERIALS CHARACTERIZATION BY NDE

The previous discussions clearly indicate that any nondestructive evaluation (NDE) methods that are sensitive to the metallurgical or physical parameters and their changes due to fatigue are highly desirable. We restrict ourselves here to methods sensitive to the first, roughly 90% of the fatigue life before large crack growth occurs. In design, critical components (such as engines) whose life is controlled by fatigue are presently supposed to be retired as soon as the probability of forming a crack of a small but finite size is 0.1%, e.g. [16], independent of whether or not such a crack actually exists. To avoid waste it is possible by NDE methods to retire only those components having cracks of specific sizes (roughly 0.5mm) [17], which is relatively late in the total fatigue life (roughly 90%). Thus, any improvement to detect microstructural damage lower than this figure requires new, sensitive and reliable NDE tools. Recent literature reviews [18-20] provide many ideas in this respect. Yang and Fatemi [19] distinguish between two types of measurements: (i) surface and subsurface damage measurements and (ii) bulk damage measurements. In many cases damage is concentrated at the surface or slightly below as evidenced by the fact that removal of the top surface layer by chemical etching restores almost the full life of the fatigued specimens. In the following, we will be discussing very briefly some of these damage measurements without making the claim that the list is complete.

Acoustic Measurements

Probably the widest range of experimental techniques to determine fatigue damage exists in the acoustic area. One particular interesting example is in the form of a modulation experiment where the acoustically applied cyclic fatigue load is superimposed by a high frequency probe signal. Figure 10 shows a simplified version under static loading indicating

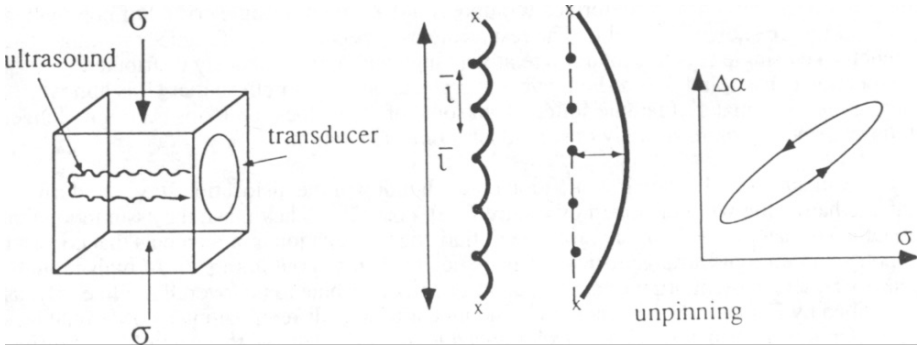

Figure 10. The effects of a bias load on the high frequency attenuation (after Ref. [21]).

dislocation breakaway (plastic yield) and the resulting effects on the attenuation [21]. Similar experiments were performed by Green [22] also noting the change of the ultrasonic attenuation due to dislocation effects.

Hikata et al. [23,24] introduced the idea that the displacement due to the bowing out of dislocations, U_d, is a contributor to harmonic generation. This U_d is determined by the Koehler-Granato-Lücke vibrating string model

$$m_d(\partial^2 U_d/\partial t^2) + B(\partial U_d/\partial t) - C(\partial^2 U_d/\partial y^2 + \ldots) = \sigma b \exp(i\omega t) \quad (5)$$

where m_d is the dislocation mass, B the damping coefficient, C the line tension, σ the stress amplitude and b the Burgers vector. This displacement U_d adds to the elastic lattice displacement, U_l, so that the equilibrium condition becomes

$$\text{div}\ \sigma = \rho\, \partial^2(U_l + U_d)/\partial t^2. \quad (6)$$

The solution of Equation 6 is very complex. A major conclusion, however, is that the third harmonic may be more sensitive to dislocation contributions than the second harmonic, as was indeed observed in some experiments [25]. The effects of fatigue on the second harmonic and

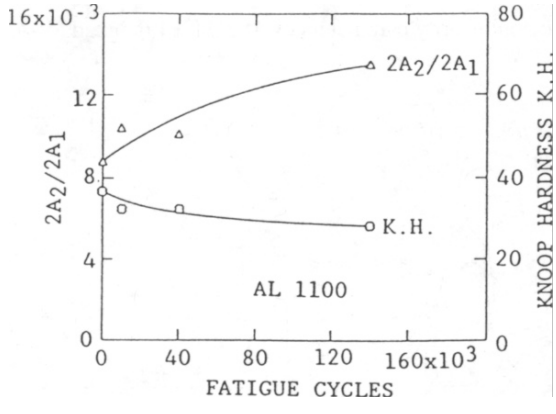

Figure 11. Second harmonic generation and Knoop hardness as a function of fatigue (after Ref. 25).

the Knoop hardness of a predeformed (compression) aluminum single crystal of nominally high purity are shown in Fig. 11. The results are as expected during fatigue softening. The predeformed single crystal contains a relatively high and homogeneously distributed dislocation density and thus a short, average dislocation loop length so that U_d is almost negligible. The material fatigue softens with some of the dislocation loops becoming longer, thus contributing more strongly to second harmonic generation.

A much more detailed investigation on the buildup of the dislocation structure during fatigue hardening was performed by Cantrell and Yost [26]. They make the assumption that in fatigued materials it is highly probable to find edge dislocation arrangements that consist of dipole and multipole arrangements as schematically sketched out in Fig. 7. At high enough shear stresses, these multipoles can break away and contribute to the overall nonlinearity, as described by Equation 6. The increase in nonlinearity with different amounts of fatigue is shown in Fig. 12 (samples 1 and 3 experienced less fatigue damage than sample 2) at different shear stress amplitudes. As a consequence of residual stress buildup during fatigue, the dislocation breakaway shifts to lower shear stresses as fatigue damage builds up. These authors find reasonable agreement between the predicted and observed enhancement of the acoustic nonlinearity.

Richardson [27] pointed out that an unbonded interface (such as a crack), subjected to a sufficiently intense incident acoustic wave, acts as a harmonic generator. Experiments on

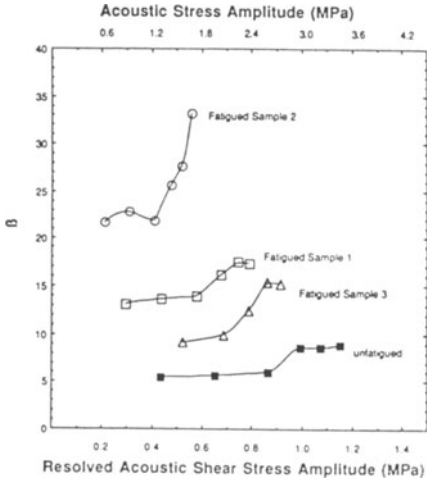

Figure 12. Acoustic nonlinearity parameters of Al2024-T4 fatigued to various damage levels (after Ref. 26).

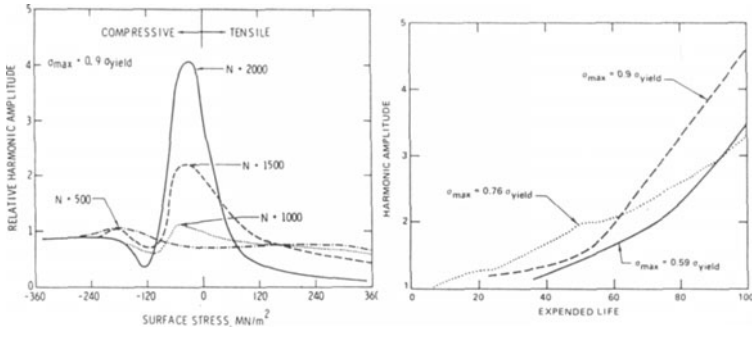

Figure 13. Dependence of harmonic generation on a) surface stress, and fatigue cycles and b) on expended life (after Ref. 28).

fatigue cracks [28] confirmed this prediction. Figures 13a and b show the harmonic generation as small fatigue cracks develop at the surface of a high strength aluminum alloy. Generation is most efficient close to a zero stress in the surface and increases with the growth of surface cracks. If the cracks are completely closed, due to a compressive stress, or fully open, due to a tension stress, harmonic generation disappears as one would expect from this model [27,29].

Acoustic Emission

Acoustic emission is often called a passive acoustic phenomenon in that only a receiver to detect the signal is required. We assume that grip and other extraneous noises, such as friction noises between crack faces, can be eliminated. The sources of true acoustic emission are clearly accelerating or decelerating dislocations or second phase particle breaking. Both events have to go fast and may be viewed as a result of phonon emission. Particularly the analysis of the dislocation dynamics is very complex [30]. Second phase particle breaking is certainly much easier to correlate with the microstructure using such methods as micrographic observations. To this author's knowledge a thorough analysis of acoustic emission during fatigue in terms of dislocation and particle events has not been performed yet. There is evidence, however, [Ref. 31, e.g.] that the acoustic emission events observed occur mostly from particle breaking during the last 10 to 20% of fatigue life, with the acoustic emission bursts depending heavily on the heat treatment of the material.

Magnetic Measurements

Magnetic measurements during fatigue also make use of a wide variety of parameters such as coercivity, remanence, maximum differential permeability, hysteresis losses, as well as acoustic and magnetic Barkhausen signals and considerable work has been reported. Figures 14a and b show some work by Govindaraju et al. [32] which shows the variation of coercivity and remanence as a function of expended fatigue life in a railroad bridge steel under low cycle fatigue conditions. In both cases during a brief period of fatigue softening (L_{max}) both coercivity and remanence increase to remain basically constant during the saturation stage of fatigue. Only during the last few percent of the life occurs a dramatic decrease in both coercivity and remanence. Surface replication has shown that micro- and macrocracks appear during this period and are the probable cause for the large load drop (compliance) and with it the drop in coercivity and remanence.

Significant efforts have been spent recently on the effects of fatigue on the magnetic Barkhausen and the magnetoacoustic effects. From a literature study it appears that both effects (and particularly the magnetic Barkhausen effect) are more sensitive to microstructural changes than coercivity and remanence due to the fact that the Blochwall thickness is of the order of about 1000Å which is typical for the short range internal stresses built up (or destroyed) during fatigue. Figure 15 shows results obtained by Le Brun and Billy [33] on the shift of the magnetic Barkhausen maximum to larger applied magnetic field as fatigue damage increases.

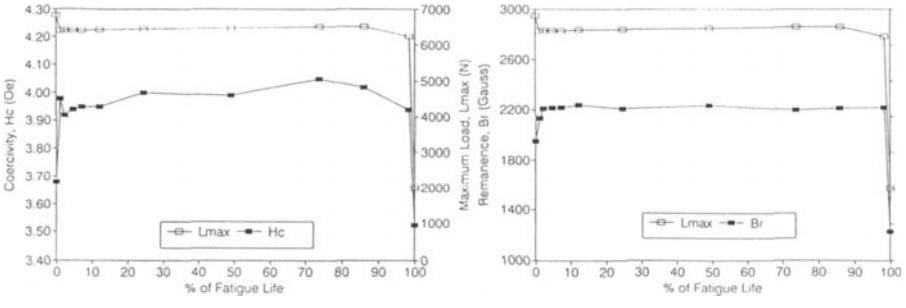

Figure 14. a) Change in coercivity and b) in remanence with fatigue life expended (after Ref. 32).

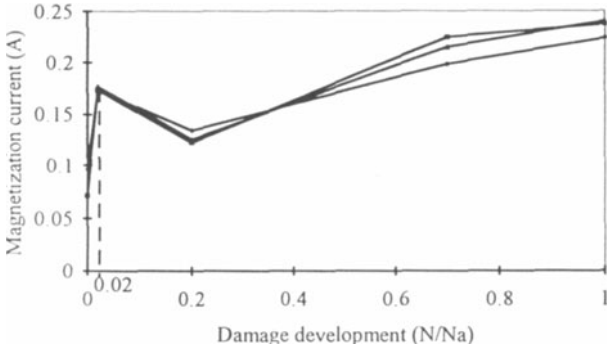

Figure 15. The change of the magnetic Barkhausen peak position as a function of fatigue damage in a turbine alloy [after Ref. 33].

Recently, the use of SQUIDs to determine magnetic property changes (remanence) has become popular. In one example [34] the aging of duplex steel has been followed successfully. This author is not aware, however, of any measurements on fatigue life as yet.

X-ray Techniques

Pangborn et al. [35] studied the dislocation distribution of fatigued specimen (such as Al 2024-T3) using X-ray double-crystal diffractometry. In all cases they noted that there is an excess dislocation density near the surface of the material followed by a trough at roughly 100μm depth after which the density increases again, but to a level that is not as high as at the surface. As shown in Fig. 16a, the ratio of "excess" dislocations at the surface to those in the "bulk" decreases substantially with fatigue (in this case low cycle fatigue). A rough estimate indicates that the two dislocation densities are about equal at failure. Fig. 16b provides sketches of X-ray rocking curves half widths as expected from the formation of extrusions-intrusions, of microcrack formation, combined effects and an ideal curve deep into the material and unaffected by fatigue.

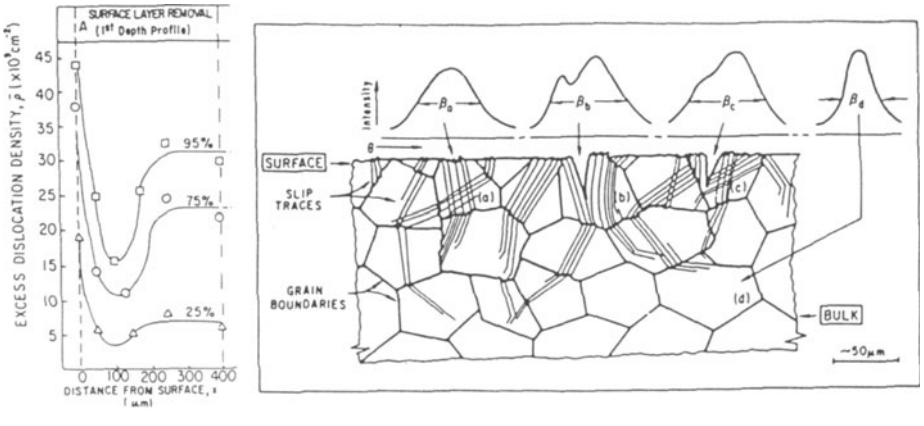

Figure 16. a) "Excess" dislocations at the surface and towards the bulk of fatigued Al 2024-T3. b) X-ray rocking curves at various surface locations. [after Ref. 35]

Optical Methods

The formation of surface roughness by extrusions/intrusions offers, for highly polished specimens, a good method to follow fatigue damage by optical methods. Haworth et al. [36] report on an optical correlation technique in which topographical information from the surface

is recorded holographically and compared with the actual surface by measuring the correlation intensity as fatigue damage accumulates. Figure 17 shows the correlation intensity as a function of fatigue cycles for Al 2024-T3. Apparently after some fatigue softening the correlation intensity shows an extended saturation range during which extrusion/intrusion and microcrack formation occurs, which is then followed by crack coalescence and macrocrack growth.

Several years ago, there was a great interest in fatigue induced photostimulated exo-electron emission (PEEE). Two clearly distinct effects of the surface of fatigued specimen have been identified [37,38]. A change in the surface topography can lead to a change of PEEE with or without an oxide layer on the surface. It was shown [37] that the roughness induced by fatigue is able to couple the incident light to surface "plasmons." These plasmons are electromagnetic waves which propagate parallel to the surface. If a resonant condition between the incident photon and the surface plasmon is met the incident photon is absorbed by the plasmon. Such an excited surface plasmon decays to an energetic single electron which increases the photocurrent. Its peak value depends on the oxide layer thickness. On the other hand [38], just putting an oxide layer on a metal, such as Al will shift the work function and be an absorber for the emitted electrons. Thus, oxide break-up during fatigue provides enhanced photoemission. Unfortunately both types of experiments have to be performd under high vacuum and therefore have never found their place in useful fatigue monitoring techniques.

Positron Annihilation

A topic that is still emerging from time to time as a possibility for monitoring of fatigue damage is positron annihilation. Even in the simplest cases a variety of defects are created that may lead to positron trapping such as vacancies, dislocations, jogs on dislocations, etc. A clear picture has not evolved, except that the mean positron lifetime at vacancies increases very rapidly during the first 7% of the fatigue life of Ni from about 90 ps to about 190 ps and then saturates at that level [39]. There are most likely vacancies created during fatigue. To another

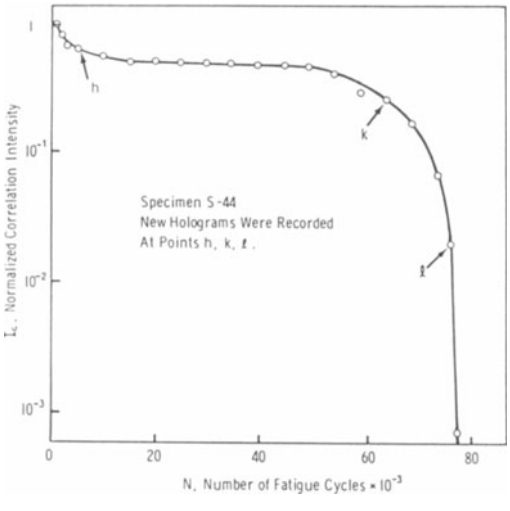

Figure 17. Correlation intensity curve for fatigued Al 2024-T3. [after Ref. 36]

conclusion came Tien et al. [40] on superalloys. In addition to the positron lifetime at vacancies, they thought to have observed a defect with a much longer positron lifetime (roughly 500 ps or larger) which only appears after deformation (fatigue) and therefore appears to be due to the dislocations. In either case, fatigue clearly has an effect on positron lifetimes although the details are not clear.

Conclusions

Fatigue is, without a doubt, one of the most costly materials degradation mechanisms. We are just now getting a more complete picture of the cradle-to-grave physical and microstructural changes that occur in the material. But we have to keep in mind that each material, at least from the microstructural point of view, behaves differently. We also have to keep in mind that fatigue is a very history dependent phenomenon. Both facts make it difficult for a plant operator to tell precisely at what state of life the component under question really is. Therefore, we are constantly searching for new physical phenomena that could tell us about the accumulated damage state of the material and therefore, under certain assumptions, its remaining life.

This author believes that there is a good number of NDE techniques that could provide us realistically with information on the state of fatigue. However, what is badly needed is a national effort in which National Labs, universities and particularly industry collaborate for a common goal. Similar recommendations have been made recently [41] at a workshop dedicated to materials property measurements in power plants.

ACKNOWLEDGEMENT

This work was performed at Ames Laboratory under Contract Number W-7405-Eng-82 with the U.S. Department of Energy.

REFERENCES

1. D. L. Davidson, J. Nondestructive Evaluation 15, 101 (1996).
2. M. E. Fine and I. B. Kwon, in *Small Fatigue Cracks*, eds. R. O. Ritchie and J. Lankford (The Metallurgical Society, Warrendale, PA, 1986), p. 29.
3. J. Lankford and D. L. Davidson, in *Small Fatigue Cracks*, eds. R. O. Ritchie and J. Lankford (The Metallurgical Society, Warrendale, PA, 1986), p. 51.
4. H. Kitagawa, S. Takahashi, C. M. Suh, and S. Miyashita, in *Fatigue Mechanisms: Advances in Quantitative Measurement of Physical Damage*, ASTM STP 675, ed. J. Fong (Am. Soc. Testing and Materials, Philadephia, PA, 1986), p. 420.
5. M. R. Mitchell, in *Fatigue and Microstructure*, ed. M. Meshii (American Society for Metals, Metals Park, OH, 1979), p. 385.
6. J. C. Grosskreutz, phys. stat. sol.(b) 47, 11 (1971).
7. J. C. Grosskreutz, phys. stat. sol.(b) 47, 359 (1971).
8. R. Chang, W. L. Morris, and O. Buck, Scripta Met. 13, 191 (1979).
9. W. L. Morris, O. Buck, and H. L. Marcus, Met. Trans. 7A, 1161 (1976).
10. B. Weiss, R. Stickler, and A. Fathulla, in *Small Fatigue Cracks*, eds. R. O. Ritchie and J. Lankford (The Metallurgical Society, Warrendale, PA, 1986), p. 471.
11. A. N. Stroh, Adv. Physics 6, 418 (1957).
12. B.-T. Ma and C. Laird, in *Small Fatigue Cracks*, eds. R. O. Ritchie and J. Lankford (The Metallurgical Society, Warrendale, PA, 1986), p. 9.
13. W. Elber, in *Damage Tolerance in Aircraft Structures*, ASTM STP 415 (Am. Soc. Testing and Materials, Philadelphia, PA, 1971), p. 230.
14. O. Buck, D. K. Rehbein, and R. B. Thompson, Eng. Fracture Mechanics 28, 413 (1987).
15. W. L. Morris, M. R. James, and O. Buck, Eng. Fracture Mechanics 13, 213 (1980).
16. J. E. Allison, J. M. Hyzak, and W. H. Reimann, in *Prevention of Structural Failures*, ed. W. Lewis (Am. Soc. for Metals, Metals Park, OH, 1978), p. 240.
17. C. G. Annis, J. S. Cargill, J. A. Harris, and M. C. Vanwanderham, in *Nondestructive Evaluation: Microstructural Characterization and Reliability Strategies*, eds. O. Buck and S. M. Wolf (The Metallurgical Society, Warrendale, PA, 1981), p. 53.

18. R. B. Thompson, J. Nondestructive Evaluation 15, 163 (1996).
19. L. Yang and A. Fatemi, accepted by J. Testing and Evaluation 26, 2.
20. G. Dobmann, in *Review of Progress in QNDE*, Vol. 14B, eds. D. O. Thompson and D. E. Chimenti (Plenum Press, New York, NY, 1995), p. 2003.
21. G. Gremaud and M. Bujard, J. de Physique 46, C10-135 (185).
22. R. E. Green, J. de Physique 46, C10-827 (1985).
23. A. Hikata and C. Elbaum, Phys. Rev. 144, 469 (1966).
24. A. Hikata, F. A. Sewell, and C. Elbaum, Phys. Rev. 151, 442 (1966).
25. O. Buck, IEEE Trans. Sonics and Ultrasonics SU-23, 346 (1976).
26. J. H. Cantrell and W. T. Yost, Phil. Mag. 69, 315 (1994).
27. J. M. Richardson, Int. J. Eng. Sci. 17, 73 (1979).
28. W. L. Morris, O. Buck, and R. V. Inman, J. Appl. Phys. 50, 6737 (1979).
29. J. D. Barnard, G. E. Dace, D. K. Rehbein, and O. Buck, J. Nondestructive Evaluation 16, 77 (1997).
30. W. W. Gerberich and K. Jatavallabhula, *in Nondestructive Evaluation: Microstructural Characterization and Reliability Strategies*, eds. O. Buck and S. M. Wolf (The Metallurgical Society, Warrendale, PA, 1981), p. 319.
31. J. C. Duke and R. E. Green, Int. J. Fatigue, 125 (July 1979).
32. M. R. Govindaraju, A. Strom, D. C. Jiles, and S. B. Biner, *in Review of Progresss in QNDE*, Vol. 12B, eds. D. O. Thompson and D. E. Chimenti (Plenum Press, New York, 1993), p. 1839.
33. A. Le Brun and F. Billy, in *Review of Progress in QNDE*, Vol. 13B, eds. D. O. Thompson and D. E. Chimenti (Plenum Press, New York, 1994), p. 1833.
34. S. Evanson, M. Otaka, and K. Hasegawa, *J. Eng. Materials and Technology* 114, 41, 1992.
35. R. N. Pangborn, S. Weissmann, and I. R. Kramer, Metall Transactions 12A, 109 (1981).
36. W. L. Haworth, A. F. Hieber, and R. K. Mueller, Metall Transactions 8A, 1597 (1977).
37. W. J. Pardee and O. Buck, Appl. Phys. 14, 376 (1977)
38. W. J. Baxter in *Electron and Positron Spectroscopies in Materials Science and Engineering*, eds. O. Buck, J. K. Tien, and H. L. Marcus (Academic Press, New York, 1979) p. 35.
39. L. Granatelli and K. G. Lynn in *Nondestructive Evaluation: Microstructural Characterization and Reliability Strategies*, eds. O. Buck and S. M. Wolf (Metallurgical Society, Warrendale, PA, 1981) p. 169.
40. J. K. Tien, S. J. Tao, J. P. Wallace, and S. Purushothaman, in *Electron and Positron Spectroscopies in Materials Sciences and Engineering,* eds. O. Buck, J. K. Tien and H. L. Marcus (Academic Press, New York, 1979) p.73.
41. O. Buck, T. T. Taylor, and G. A. Alers, J. Nond. Evaluation 15, 89 (1996).